J|A|C|S
COMMUNICATIONS

Extraordinarily High Zr^{4+} Ion Conducting Solid

Nobuhito Imanaka,* Shinji Tamura, and Tetsushi Itano

Department of Applied Chemistry, Faculty of Engineering, Osaka University,
2-1 Yamadaoka, Suita, Osaka 565-0871, Japan

Received January 15, 2007; E-mail: imanaka@chem.eng.osaka-u.ac.jp

Until now, many types of solid electrolytes that conduct mono- and divalent ions have been developed since 1838,[1] and some of these electrolytes are expected to be applied to electrical devices, such as rechargeable batteries (Li^+ ion conductor[2]), fuel cells (H^+[3] or O^{2-} ion conductors[4]), and chemical sensors (many kinds of cation and anion conductors). However, they have a potential disadvantage in lower chemical stability (e.g., explosive accidents for Li^+ ion batteries and deterioration in gas sensing with monovalent ion conductor[5]) when compared with higher valency ionic conductors that are composed of only tri-, tetra-, penta-, and hexavalent cations. Therefore, if a solid electrolyte with high-ionic conductivity is developed by selecting only such high-valency ions, it would be a superior candidate for new types of components for various devices. In 1995, the field of solid electrolyte research experienced a discovery of a trivalent ion conductor of Sc^{3+} ion conducting $Sc_2(WO_4)_3$ solid.[6] Since this discovery, a variety of trivalent cation conductors have been reported.[7−10] Although tetravalent Zr^{4+} ion conductions in $Zr_2O(PO_4)_2$,[11] $ZrNb(PO_4)_3$, and $ZrM(PO_4)_3$ (M = Nb and Ta)[12] have been reported since the year 2000, the Zr^{4+} ion conductivities in these solids were still appreciably lower ($<10^{-4}$ $S{\cdot}cm^{-1}$) than that for mono- and divalent cations ($>10^{-4}$ $S{\cdot}cm^{-1}$), so that the enhancement of the Zr^{4+} ion conductivity will be required for successful application in such electrical devices. Here, we report two potential ways for improving the Zr^{4+} ion conduction in crystalline solids: one is the expansion of the ion conduction pathway in the structure and the other is the reduction of strong electrostatic interactions between the conducting Zr^{4+} ion and the surrounding counter O^{2-} anions.

In this Communication, we selected W^{6+} having larger ionic size (ionic radius: 0.056 nm [coordination number (CN): 4][13]) and also higher valence compared to P^{5+} (0.031 nm [CN: 4][13]) as a key cation for realizing the above-mentioned two potential ways simultaneously. Zr^{4+} ion conducting properties of the $Zr_{1-x/4}TaP_{3-x}W_xO_{12}$ solid, where the P^{5+} sites in NASICON[14]-type $ZrTa(PO_4)_3$ were partially replaced with W^{6+}, were investigated.

From the X-ray powder diffraction (XRD) analyses of the $Zr_{1-x/4}TaP_{3-x}W_xO_{12}$ ($0.0 \leq x \leq 0.2$) solids prepared, it was found that single phase NASICON-type structures were successfully obtained for the samples with $x < 0.15$, and the lattice volume linearly increased with increase in x.[15] In contrast, the samples with $x \geq 0.15$ resulted in a two phase mixture of NASICON-type phosphate and $TaPO_5$, without any lattice expansion of the NASICON-type phase compared with the case for the single phase sample ($x = 0.1$). These results clearly indicate that the solid solubility limit for W^{6+} on P^{5+} sites is ca. $x = 0.1$.

Figure 1 displays the compositional dependence of the electrical conductivity at 873 K for the $Zr_{1-x/4}TaP_{3-x}W_xO_{12}$ solids ($0.0 \leq x \leq 0.2$). The conductivity monotonically increases with increase in the W content (x) within the single phase region ($x \leq 0.1$), and $Zr_{39/40}TaP_{2.9}W_{0.1}O_{12}$ ($x = 0.1$) shows the highest conductivity of 4.7×10^{-4} $S{\cdot}cm^{-1}$, which enters into the practical application range ($>10^{-4}$ $S{\cdot}cm^{-1}$). In the two-phase mixture region ($x > 0.1$), the conductivity was drastically reduced in comparison with that for the sample with $x = 0.1$. A significant reduction in conductivity that appeared between the compositions at $x = 0.10$ and 0.15 is ascribed to the formation of low-conductive $TaPO_5$ (the conductivity of $TaPO_5$ is depicted in Figure 3), which prevents Zr^{4+} ion conduction in the solids. (The direct demonstration of Zr^{4+} ion conduction in $Zr_{39/40}TaP_{2.9}W_{0.1}O_{12}$ ($x = 0.1$) is described below.) This phenomenon also supports the idea that the compositional limit for obtaining the single-phase NASICON-type structure is $x = 0.1$.

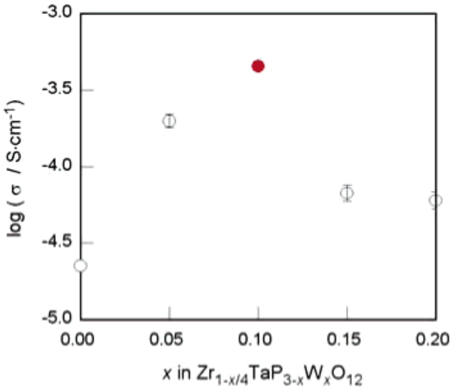

Figure 1. Compositional dependence of the electrical conductivity of $Zr_{1-x/4}TaP_{3-x}W_xO_{12}$ ($0.0 \leq x \leq 0.2$) at 873 K.

For the purpose of identifying the conducting species in the $Zr_{39/40}TaP_{2.9}W_{0.1}O_{12}$ solid, which shows the highest conductivity among the samples prepared, the polarization behavior was investigated by measuring the time-dependent dc to ac conductivity ratio (σ_{dc}/σ_{ac}) in oxygen (P_{O2}: 10^5 Pa) and helium (P_{O2}: 12 Pa) atmospheres at 873 K. This method can provide information as to the type of charge carrier conduction in the solid.[6] The σ_{dc}/σ_{ac} ratio was reduced to values less than 0.005 in both atmospheres after 30 min, which suggests that the conducting species in the $Zr_{39/40}TaP_{2.9}W_{0.1}O_{12}$ solid is limited to cationic species, that is, Zr^{4+}, Ta^{5+}, P^{5+}, and W^{6+}. To directly demonstrate Zr^{4+} ion conduction in the $Zr_{39/40}TaP_{2.9}W_{0.1}O_{12}$ solid, dc electrolysis was carried out by applying a dc voltage of 4 V for 380 h at 923 K, which is higher than the decomposition voltage of ca. 1.4 V. Here, the dc electrolysis was conducted at 923 K, which was 50 K higher than that for the above polarization measurement to shorten the electrolysis period by enhancing the Zr^{4+} ion conductivity. By applying a dc voltage higher than the decomposition voltage, only the conducting cation species is forced to continuously and macroscopically migrate toward the cathodic direction, and as a result, evidence of the migration of the conducting cationic species can be found at or near the cathodic surface. After the dc electrolysis, line electron probe microanalysis (EPMA) measurements of the electrolyzed pellet were performed, and the results are depicted in Figure 2. A clear segregation was observed only for Zr near the cathodic surface.

10.1021/ja070293x CCC: $37.00 © 2007 American Chemical Society

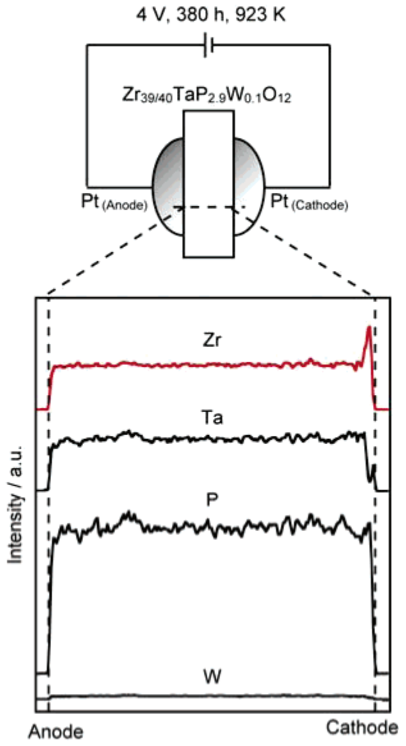

Figure 2. Setup for dc electrolysis and the EPMA line analysis result for cationic species in the $Zr_{39/40}TaP_{2.9}W_{0.1}O_{12}$ solid.

Zr segregation inside of the sample pellet indicates that Zr^{4+} migrated from the anodic side through the sample and was not generated by sample decomposition at the cathodic surface. This result clearly demonstrates that only Zr^{4+} ion migration occurs in $Zr_{39/40}TaP_{2.9}W_{0.1}O_{12}$. Furthermore, the cation transference number is estimated to be higher than 0.995 from the σ_{dc}/σ_{ac} ratio after 30 min, so that it is clear the conducting species in $Zr_{39/40}TaP_{2.9}W_{0.1}O_{12}$ is only the tetravalent Zr^{4+} ion.

The temperature dependence of Zr^{4+} ion conductivity for the $Zr_{39/40}TaP_{2.9}W_{0.1}O_{12}$ solid is shown in Figure 3 with the corresponding data for $ZrTa(PO_4)_3$, $TaPO_5$, and representative conductivities for the divalent oxide anion in yttria stabilized zirconia (YSZ) and calcia stabilized zirconia (CSZ),[4] which have already been applied as oxygen-gas detecting elements of commercialized oxygen sensors used in the automobile and steel industry fields. The Zr^{4+} ion conductivity of $Zr_{39/40}TaP_{2.9}W_{0.1}O_{12}$ at 873 K was approximately 19 times as high as that of $ZrTa(PO_4)_3$, and the value is comparable to those of practically utilized divalent oxide anion conducting YSZ and CSZ. The average activation energy (48.7 $kJ{\cdot}mol^{-1}$ at a temperature range between 723 and 873 K) for Zr^{4+} ion conduction in $Zr_{39/40}TaP_{2.9}W_{0.1}O_{12}$ is lower than that in $ZrTa(PO_4)_3$ (55.9 $kJ{\cdot}mol^{-1}$ at same temperature range), indicating that smooth Zr^{4+} ion conduction in the NASICON-type structure is realized for the $Zr_{39/40}TaP_{2.9}W_{0.1}O_{12}$ solid by expansion of the NASICON-type crystal lattice. In addition, the higher valence state of W^{6+} over P^{5+} is effective for enhancement of the Zr^{4+} ion conductivity and lowering of the activation energy, because the electrostatic interactions between the mobile Zr^{4+} cations and surrounding O^{2-} anions are reduced by the enlargement of the effective valence state of (P, W), which attracts the O^{2-} ions surrounding mobile Zr^{4+} ions in addition to expanding the NASICON crystal lattice.

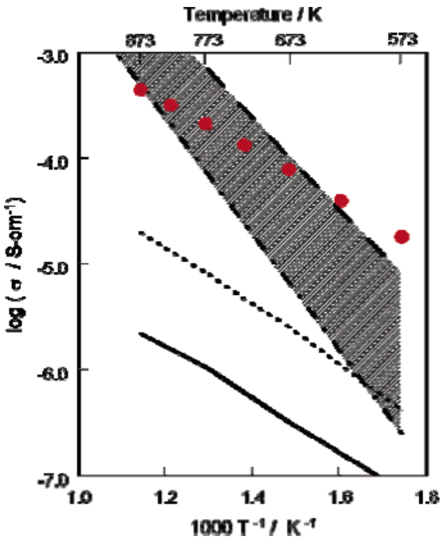

Figure 3. Temperature dependency of the electrical conductivity for $Zr_{39/40}TaP_{2.9}W_{0.1}O_{12}$ (●), $ZrTa(PO_4)_3$ (•••), and $TaPO_5$ (—) with the conductivity region of representative divalent oxide ion conducting stabilized zirconias (shaded area; YSZ (---) and CSZ (-•-•-)).

Acknowledgment. Present work was partially supported by the Industrial Technology Research Grant Program in ’05 (Project ID: 05A18011d) from the New Energy and Industrial Technology Development Organization (NEDO) of Japan. This work was also supported by a Grant-in-Aid for Science Research (No. 17750196) from the Ministry of Education, Science, Sports and Culture.

Supporting Information Available: Experimental procedures and Figures S0 and S1. This material is available free of charge via the Internet at http://pubs.acs.org.

References

(1) Faraday, M. *Philos. Trans. R. Soc. London* **1838**.
(2) For example: Hong, H. Y.-P. *Mater. Res. Bull.* **1978**, *13*, 117−124.
(3) For example: Iwahara, H.; Esaka, T.; Uchida, H.; Maeda, N. *Solid State Ionics* **1981**, *3/4*, 359−363.
(4) For example: Strickler, D. W.; Carlson, W. G. *J. Am. Ceram. Soc*. **1964**, *47*, 122−127.
(5) Tamura, S.; Imanaka, N.; Kamikawa, M.; Adachi, G. *Sens. Actuators B* **2001**, 73, 205−210.
(6) Imanaka, N.; Kobayashi, Y.; Adachi, G. *Chem. Lett.* **1995**, *24*, 433−434.
(7) Kobayashi, Y.; Egawa, T.; Tamura, S.; Imanaka, N.; Adachi, G. *Chem. Mater*. **1997**, *9*, 1649−1654.
(8) Imanaka, N.; Tamura, S.; Hiraiwa, M.; Adachi, G.; Dabkowska, H.; Dabkowski, A.; Greedan, J. E. *Chem. Mater*. **1998**, *10*, 2542−2545.
(9) Tamura, S.; Imanaka, N.; Adachi, G. *Adv. Mater*. **1999**, *11*, 1521−1523.
(10) Imanaka, N.; Hasegawa, Y.; Yamaguchi, M.; Itaya, M.; Tamura, S.; Adachi, G. *Chem. Mater*. **2002**, *14*, 4481−4483.
(11) Imanaka, N.; Ueda, T.; Okazaki, Y.; Tamura, S.; Hiraiwa, M.; Adachi, G. *Chem. Lett.* **2000**, *29*, 452−453.
(12) Imanaka, N.; Ueda, T.; Adachi, G. *J. Solid State Electrochem*. **2003**, *7*, 239−243.
(13) Shannon, R. D. *Acta Cryst.* **1976**, *A32*, 751−767.
(14) Goodenough, J. B.; Hong, H. Y.-P.; Kafalas, J. A. *Mater. Res. Bull*. **1976**, *11*, 203−220.
(15) See Supporting Information.

JA070293X